Adsorption Properties of Hydrogen and Carbon Dioxide in Prussian Blue Analogues M3[Co(CN)6]2, M = Co, Zn

ARTICLE *in* THE JOURNAL OF PHYSICAL CHEMISTRY C · DECEMBER 2006

Impact Factor: 4.77 · DOI: 10.1021/jp065845x

4 AUTHORS, INCLUDING:

Sittichai Natesakhawat
National Energy Technology Laboratory
31 PUBLICATIONS **777** CITATIONS

SEE PROFILE

Adsorption Properties of Hydrogen and Carbon Dioxide in Prussian Blue Analogues $M_3[Co(CN)_6]_2$, M = Co, Zn

Sittichai Natesakhawat,* Jeffrey T. Culp, Christopher Matranga, and Bradley Bockrath

National Energy Technology Laboratory, United States Department of Energy, P.O. Box 10940, Pittsburgh, Pennsylvania 15236

Received: September 7, 2006; In Final Form: October 17, 2006

H_2 and CO_2 adsorption were studied in dehydrated Prussian blue analogues $M_3[Co(CN)_6]_2$ (M = Co, Zn) using volumetric isotherm measurements. Both materials adsorbed 1.2−1.3 wt % of H_2 at 77 K and 760 Torr with isosteric heats of adsorption ranging from 5.9 to 6.8 kJ/mol. High-pressure H_2 isotherms at 77 K showed that $Co_3[Co(CN)_6]_2$ started to saturate well above 6 atm with a saturation coverage of ∼1.9 wt %. These materials adsorbed approximately 17.6−19.7 wt % of CO_2 at 253 K and 760 Torr with isosteric heats of adsorption of ∼25−28 kJ/mol. The CO_2 saturation coverages from high-pressure isotherms at 263 K and 15 atm were ∼27.4−29.0 wt %. The displacement of CO_2 by H_2 in these compounds was investigated with Fourier transform infrared spectroscopy (FTIR). The FTIR experiments showed that CO_2 physisorption at cryogenic temperatures produced an infrared peak at 2335 cm^{-1}. Co-adsorption experiments revealed that H_2 was able to displace preadsorbed CO_2 if the P_{H2}/P_{CO2} ratio was well above 100. The infrared results from the co-adsorption experiments also showed that H_2 and CO_2 competed for adsorption in the same pores under these conditions.

Introduction

In this paper, we report the adsorption properties of H_2 and CO_2 in $Co_3[Co(CN)_6]_2$ and $Zn_3[Co(CN)_6]_2$ Prussian blue analogues. We find that H_2 is capable of displacing preadsorbed CO_2 for P_{H2}/P_{CO2} ratios in excess of 100. Our results indicate that in addition to the promising H_2 storage materials reported in the literature,[1−3] these Prussian blue analogues have properties that may be useful for CO_2 storage and separation applications.

Our interest in this class of materials has been stimulated by recent literature which found that several Prussian blue analogues stored ∼1.2−1.4 wt % of H_2 at 77 K and 760 Torr.[1,2] The structurally similar $Ni[Fe(CN)_5NO]$ and $Co[Fe(CN)_5NO]$ metal nitroprussides also took up ∼1.6 wt % of H_2 under nearly identical conditions.[4] The isosteric heats of adsorption for H_2 in the Prussian blue and metal nitroprusside materials were ∼7 kJ/mol which was ∼40% higher than what was typically observed in metal organic frameworks such as MOF-5.[1,4] The small pore sizes (∼5−10 Å), large isosteric heats, and the capability to engineer the adsorption sites into these materials make them as promising as many of the metal organic frameworks currently being evaluated as gas storage materials.[1,4]

The nanoporous Prussian blue analogues $M_3[Co(CN)_6]_2$ (M = Cd, Co, Cu, Fe, Mn, Ni, Zn) are constructed from octahedral $Co^{III}(CN)_6^{3-}$ complexes which are bridged into a simple cubic lattice by M^{2+} ions. This creates a crystal consisting of alternating M^{2+} and Co^{3+} ions connected through cyanide linkers resulting in "defect-free" pores without any unsaturated metal centers (Figure 1).[5] The charge imbalance between the $[Co^{III}(CN)_6]^{3-}$ complex and the M^{2+} ions causes disordered $[Co^{III}(CN)_6]^{3-}$ vacancies to occur at one-third of the Co^{3+} sites to maintain charge neutrality in the crystal. These vacancies are responsible for a second type of pore in the crystal (defect pore) with coordinatively unsaturated metal centers. These unsaturated metal centers crystallize with waters of hydration which are easily removed by heating to 350−425 K. The unsaturated metal centers present in these materials have been hypothesized as high-binding energy sites for hydrogen.[1]

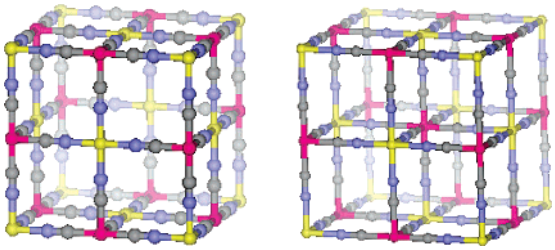

Figure 1. Structure of Prussian blue analogues $M_3[Co(CN)_6]_2$ (M = Co, Zn) showing two pore environments: the large pores created in one-third of the unit cells because of $Co(CN)_6$ vacancies (left) and the smaller pores present in the remaining defect-free unit cells (right). The −M−N≡C−Co−C≡N−M− cell edge is ∼10 Å. Key: M (yellow), Co (red), N (blue), and C (gray). Cell parameters were taken from Mullica et al.[5]

In addition to H_2 adsorption properties, the adsorption of CO_2 in H_2 sorbents is equally important since any gas stream produced by the water−gas shift (WGS) reaction will contain at least trace amounts of CO_2. In many cases, the competitive adsorption of two gases in a sorbent can be exploited for pressure-swing adsorption (PSA) applications which are commonly used for purifying mixed CO_2 and H_2 gas streams. In this regard, we have been motivated to examine CO_2 adsorption in these Prussian blue materials to better understand how they can be utilized for CO_2 storage and separation applications.

Experimental Section

Materials. The detailed synthesis procedure for Prussian blue analogues $M_3[Co(CN)_6]_2$ (M = Co, Zn) has been reported

* Author to whom correspondence should be addressed. Phone: 412-386-5096. Fax: 412-386-5920. E-mail: Sittichai.Natesakhawat@netl.doe.gov.

10.1021/jp065845x CCC: $37.00
Published on Web 12/05/2006

elsewhere.[1] Briefly, a 0.1 M aqueous solution of $K_3[Co(CN)_6]$ was added dropwise in a stirred 0.18 M aqueous solution of metal nitrate. The resulting precipitate was aged, filtered, washed, and dried in air. X-ray diffraction (XRD) patterns of these materials were obtained with a PANalytical X'Pert Pro MPD powder diffractometer using Cu Kα radiation operated at 40 kV and 40 mA. The XRD patterns were compared with JCPDS mineral powder diffraction file and matched well with those of Prussian blue-type structure. The high stability of the cyanobridged framework was also verified as indicated by nearly identical XRD patterns obtained after gas sorption measurements.

Gas Sorption Measurements. Sorption isotherms ($10^{-6}-1$ atm) of N_2, H_2, and CO_2 were collected using a Quantachrome Autosorb-1-C analyzer. Prior to the measurements, samples (120−130 mg) were degassed under vacuum at 368 K overnight. BET surface areas and total pore volumes of the samples were determined from N_2 adsorption isotherms at 77 K. Multipoint BET measurements were done at relative pressures (P/P_o) in the range of 0.1−0.3. H_2 sorption measurements were performed at 77 and 87 K. CO_2 adsorption isotherms were conducted in the temperature range of 253−303 K. The H_2 and CO_2 adsorption isotherms at high pressures were collected using a pressure−composition isotherm measurement system (Advanced Materials Corporation). This volumetric instrument is capable of collecting isotherms at a wide range of pressures (0.01−200 atm) and temperatures (77−1173 K). Approximately 500−600 mg of sample was used for high-pressure isotherm measurements. All the gases used in these experiments were ultrahigh purity grade.

Infrared Studies. FTIR experiments were conducted in a stainless steel vacuum chamber coupled to a Nicolet Nexus 670 Fourier transform infrared spectrometer equipped with an MCT detector.[6] The sample in the vacuum chamber was cooled with a continuous flow LN_2/LHe cryostat (ST-400 Model, Janis Research). All measurements were taken in the transmission geometry. Samples were dispersed on a 12.7-mm diameter, 1-mm-thick CaF_2 window (Janos Technology). The thickness of the samples was adjusted to yield an optical density of ~0.7−0.9 at 2300 cm^{-1}. Spectra for each experiment were averaged over 50 scans at a 4 cm^{-1} resolution in the 4000−650 cm^{-1} region. Prior to the collection of spectra, the samples were vacuum degassed overnight at 368 K, resulting in a base pressure of 1.0×10^{-8} Torr or lower. The removal of water was confirmed with infrared spectroscopy showing the disappearance of bands at 3700−3200 (broad) and 1615 cm^{-1} which are attributed to physisorbed water.[7−9] After degassing, the optical density of the sample was usually reduced to ~0.1−0.3 at 2300 cm^{-1} because of loss of material from the window caused by the heating step. After the degassing step, the samples were cooled to a desired temperature and were allowed to reach thermal equilibrium for 30 min. Sample dosing was done by closing the gate valve between the chamber and the pumping system while simultaneously backfilling with CO_2 (99.999%, Butler Gas) until an equilibrium pressure had been obtained. The CO_2 pressure in the system was increased incrementally and infrared measurements were taken until the samples were saturated with CO_2 (see below). Displacement of CO_2 by H_2 in dehydrated Prussian blue analogues was then performed by backfilling the chamber with H_2 (99.999%, Butler Gas) to 1.0 Torr. After backfilling, the CO_2 ν_3 (asymmetric stretching) band intensity was monitored with time and temperature. The experiments were repeated three times at each temperature to ensure data reproducibility.

TABLE 1: Summary of Adsorption Properties

material	S_{BET}[a] (m^2/g)	V_p[b] (cm^3/g)	n_{H_2}[c] (wt %)	n_{CO_2}[d] (wt %)	H_2 per u.c.	CO_2 per u.c.
$Co_3[Co(CN)_6]_2$	692	0.422	1.3	19.7	7.6	5.0
$Zn_3[Co(CN)_6]_2$	609	0.371	1.2	17.6	7.1	5.4

[a] BET surface area from N_2 at 77 K. [b] Total pore volume calculated from N_2 at 77 K and $P/P_o = 0.95$. [c] Measured at 77 K and 760 Torr. [d] Measured at 253 K and 760 Torr. The numbers of H_2 and CO_2 molecules per unit cell are calculated from saturation coverages obtained from high-pressure isotherms at 77 and 263 K, respectively. For $Zn_3[Co(CN)_6]_2$, the number of H_2 molecules per unit cell is calculated from the saturation coverage predicted from the L-F fit.

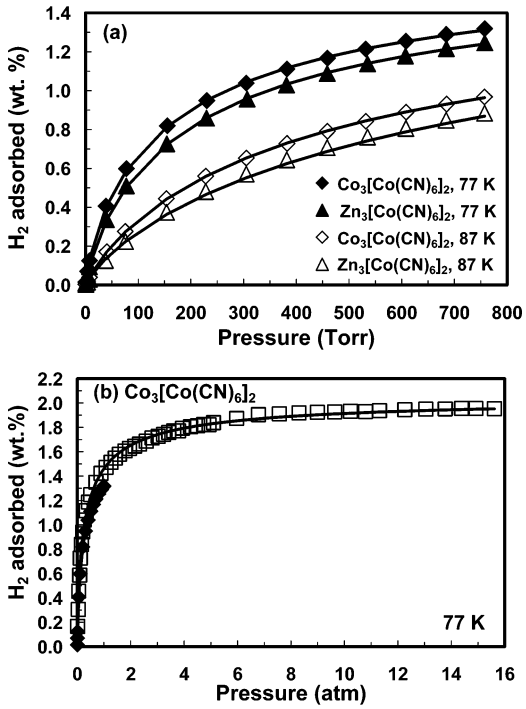

Figure 2. (a) H_2 adsorption isotherms ($10^{-6}-1$ atm) for $M_3[Co(CN)_6]_2$ (M = Co, Zn) at 77 and 87 K. (b) Comparison of H_2 adsorption isotherms collected at 77 K on $Co_3[Co(CN)_6]_2$ at low and high pressures. Solid lines through the data points are fits to the Langmuir−Freundlich (L-F) equation.

We can only monitor the CO_2 band intensity to indicate whether displacement is occurring. Gas-phase H_2 is obviously not infrared active since it is a homonuclear diatomic molecule. Physisorption inside the pores of the Prussian blue analogues did not perturb the molecule enough to make the intermolecular stretch infrared active. This prevented us from monitoring H_2 adsorption directly.

Results and Discussion

Equilibrium Adsorption Isotherms of H_2 and CO_2. The BET surface areas and pore volumes for the dehydrated $Co_3[Co(CN)_6]_2$ and $Zn_3[Co(CN)_6]_2$ samples are listed in Table 1. The surface areas are similar to previous Ar BET measurements reported by Kaye and Long.[1] The pore volumes are slightly larger than what has been noted in the structurally similar metal nitroprussides.[4]

The H_2 adsorption isotherms ($10^{-6}-1$ atm) for $Co_3[Co(CN)_6]_2$ and $Zn_3[Co(CN)_6]_2$ are shown in Figure 2a. All the H_2 isotherms are Type I which is characteristic of microporous materials. The H_2 uptake is seen to decrease with increasing temperature from 77 to 87 K indicating a physisorption-type interaction. Additionally, the H_2 uptake is fully reversible as confirmed by a

lack of hysteresis in H_2 desorption isotherms (not shown). The H_2 uptakes measured at 77 K and 760 Torr are 1.2 and 1.3 wt % for $Zn_3[Co(CN)_6]_2$ and $Co_3[Co(CN)_6]_2$, respectively. The isotherms in Figure 2a were fit to the Langmuir−Freundlich (L-F) equation so that saturation coverages could be estimated. These fits also allowed for a smooth interpolation between experimental data points for isosteric heat calculations (see below). The L-F equation is given by

$$\frac{Q}{Q_m} = \frac{BP^{1/t}}{1 + BP^{1/t}} \quad (1)$$

where Q and Q_m are the amount adsorbed at any pressure and at saturation, respectively. P is pressure. B and t are constants. The $M_3[Co(CN)_6]_2$ materials crystallize in the cubic space group $Fm3m$. However, the one-third vacancy of the $[Co^{III}(CN)_6]^{3-}$ complex, which arises because of the charge mismatch between the two ions, results in an average occupancy of 1.3333 formula units per unit cell.[5] Thus, the mass of the unit cell is 1.333 times the formula weight. The L-F equation predicts saturation coverages H_2 of ∼1.7 wt % for both $Co_3[Co(CN)_6]_2$ and $Zn_3[Co(CN)_6]_2$. This corresponds to ∼7 H_2 molecules per unit cell (i.e., ∼5.3 H_2 molecules per empirical formula unit) which is close to ∼9 H_2 molecules per unit cell predicted for structurally similar metal nitroprussides.[4] Figure 2b shows that $Co_3[Co(CN)_6]_2$ starts to saturate well above 6 atm, giving the saturation coverage of ∼1.9 wt % which is ∼10% higher than what is predicted from the L-F equation. This slight difference illustrates that if an accurate saturation coverage is required the value should be determined experimentally instead of relying solely on low-pressure extrapolations. Other authors have commented on the importance of determining saturation coverages experimentally.[10] Overall, our H_2 isotherm results are in good agreement with those values reported by Kaye and Long[1] and by Chapman et al.[2] illustrating the reproducibility of their measurements.

The CO_2 adsorption isotherms (10^{-6}−1 atm) for both compounds at 253, 263, 273, 283, and 293 K are displayed in Figure 3a and b. $Co_3[Co(CN)_6]_2$ and $Zn_3[Co(CN)_6]_2$ show Type I isotherms as observed with H_2. The CO_2 uptakes measured at 253 K and 760 Torr are 17.6 and 19.7 wt % for $Zn_3[Co(CN)_6]_2$ and $Co_3[Co(CN)_6]_2$, respectively. These values correspond to 3.3−3.6 CO_2 molecules per unit cell (i.e., 2.5−2.7 CO_2 molecules per empirical formula unit). The L-F equation estimates CO_2 saturation coverages of 30.2−30.9 wt % which equates to ∼5.7 CO_2 molecules per unit cell which seems reasonable on the basis of the estimates from the H_2 data.

CO_2 isotherms were also collected at up to 15 atm to determine the saturation coverage and to compare it to those predicted from the low-pressure data. As shown in Figure 3c and d, both compounds possess very similar CO_2 uptakes at the same temperatures. More importantly, they seem to saturate very close to the low-pressure saturation estimates provided by the L-F fits (i.e., 29.6−31.0 wt % CO_2 at 263 K).

Isosteric Heats of Adsorption (q_{st}). Information regarding the nature of the surface, site heterogeneity, and adsorbate−adsorbent interactions can be obtained from the isosteric heat of adsorption and its variation with coverage.[11] The isosteric heat of adsorption at a fixed coverage (n) can be calculated using the following relation:

$$q_{st} = -\Delta H_{ads} = R\left[\frac{\partial \ln P}{\partial (1/T)}\right]_n \quad (2)$$

where R is the gas constant, P is pressure, and T is temperature.

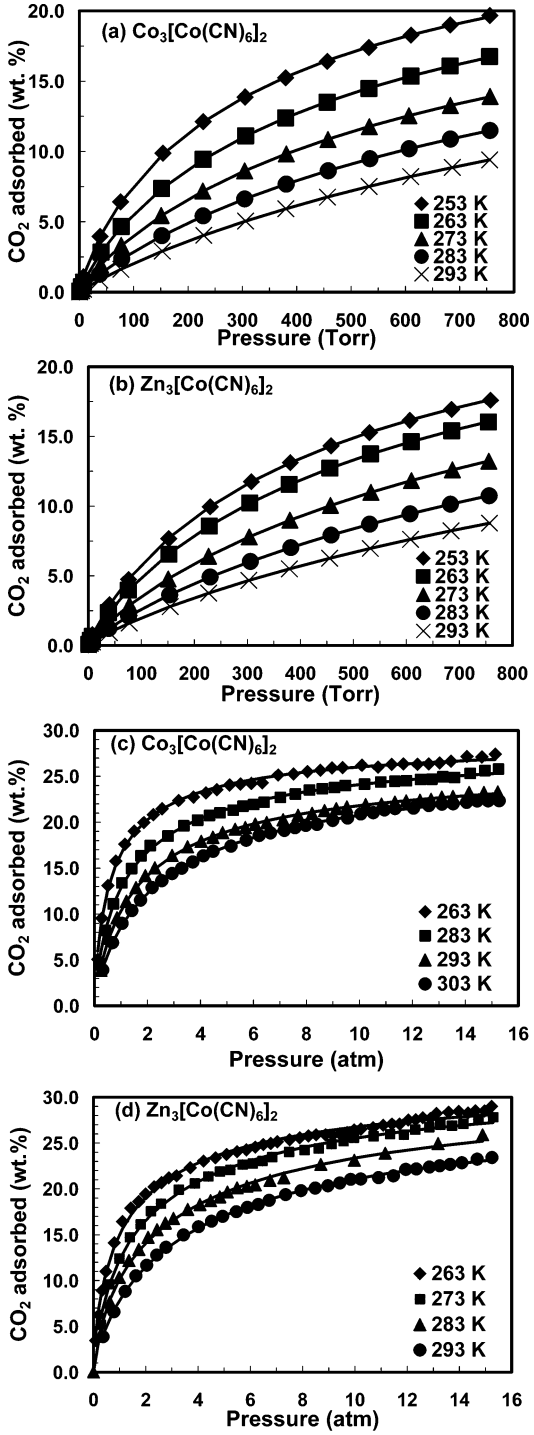

Figure 3. CO_2 adsorption isotherms (10^{-6}−1 atm) for (a) $Co_3[Co(CN)_6]_2$ and (b) $Zn_3[Co(CN)_6]_2$. CO_2 adsorption isotherms (0−15 atm) for (c) $Co_3[Co(CN)_6]_2$ and (d) $Zn_3[Co(CN)_6]_2$. Solid lines through the data points are fits to the Langmuir−Freundlich (L-F) equation.

The differential enthalpy (ΔH_{ads}) of adsorption is a negative quantity since adsorption is an exothermic process. The isosteric heat is equal in magnitude but is opposite in sign to differential enthalpy indicating that a larger and more positive isosteric heat correlates to a more strongly bound molecule.[12]

Figure 4a shows the calculated isosteric heats from adsorption data at 77 and 87 K as a function of the amount of H_2 adsorbed for $Co_3[Co(CN)_6]_2$ and $Zn_3[Co(CN)_6]_2$. The isosteric heat is nearly constant at coverages higher than 0.4 wt % of H_2 with values of 5.9−6.3 kJ/mol for $Zn_3[Co(CN)_6]_2$ and 6.4−6.8 kJ/

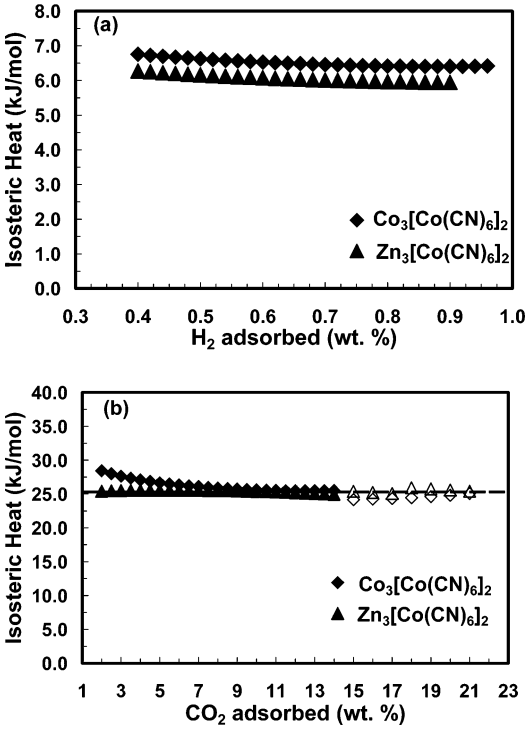

Figure 4. Calculated isosteric heat of adsorption as a function of coverage (a) H_2 and (b) CO_2. Unfilled legends show isosteric heats calculated from high-pressure CO_2 data. The dashed line represents the sublimation heat for solid CO_2.

mol for $Co_3[Co(CN)_6]_2$. Our results agree very well with previous observations reported by Kaye and Long.[1]

Figure 4b shows the isosteric heat of CO_2 adsorption calculated from the slopes of isosteres (i.e., ln P vs $1/T$ plots, see Supporting Information). The isosteric heat at coverages between 2 and 14 wt % of CO_2 is ~25 kJ/mol for $Zn_3[Co(CN)_6]_2$ and ~25−28 kJ/mol for $Co_3[Co(CN)_6]_2$. At higher coverages up to 21 wt %, the isosteric heat for both compounds seems to be nearly constant at the value of ~25 kJ/mol (unfilled legends) which is close to the sublimation heat for solid CO_2 (25.3 kJ/mol, dash line in figure).[13] Moreover, the isosteric heat of CO_2 adsorption is significantly higher than that of H_2, indicative of a stronger interaction of CO_2 molecules with the pore walls. The isosteric heats of adsorption for CO_2 from our measurements can be compared to those published in the literature for other microporous materials: 20−28 kJ/mol for silicalite;[14,15] 25 kJ/mol for Cu−BTC,[13] BTC = benzene-1,3,5-tricarboxylate; 27 kJ/mol for H−ZSM-5 zeolites;[16] 34.3 kJ/mol for $Cu_2(pzdc)_2pyz$.[17]

Infrared Studies of CO_2 Adsorption and Displacement. We have also employed FTIR to investigate CO_2 physisorption and to monitor its displacement by H_2 in Prussian blue analogues. Infrared spectra for CO_2 adsorbed on dehydrated $Zn_3[Co(CN)_6]_2$ and $Co_3[Co(CN)_6]_2$ are shown in Figure 5a and b, respectively. An infrared peak is seen at 2335 cm^{-1} after the sample is exposed to CO_2. This peak can be attributed to the asymmetric stretching mode (ν_3) of physisorbed CO_2. The spectral feature is red-shifted in comparison to the value of 2349 cm^{-1} reported for gas-phase CO_2 which indicates a significant interaction with the adsorption site.[18,19] The 2335 cm^{-1} value is comparable to the 2330−2340 cm^{-1} range of values seen in our previous studies of physisorbed CO_2 in single-walled carbon nanotubes.[6,20−24] It is also comparable to values seen for CO_2 adsorbed in C_{60} films (2328−2331 cm^{-1}),[25,26] powdered carbon (2332 cm^{-1}),[27] coal samples (2332−2335 cm^{-1}),[28] and graphite[26] (2341 cm^{-1}). The CO_2 peak grows in intensity with increasing CO_2 pressure until it saturates. This is clearly illustrated by a nearly constant value of CO_2 intensity being obtained with increasing CO_2 pressure (insets).

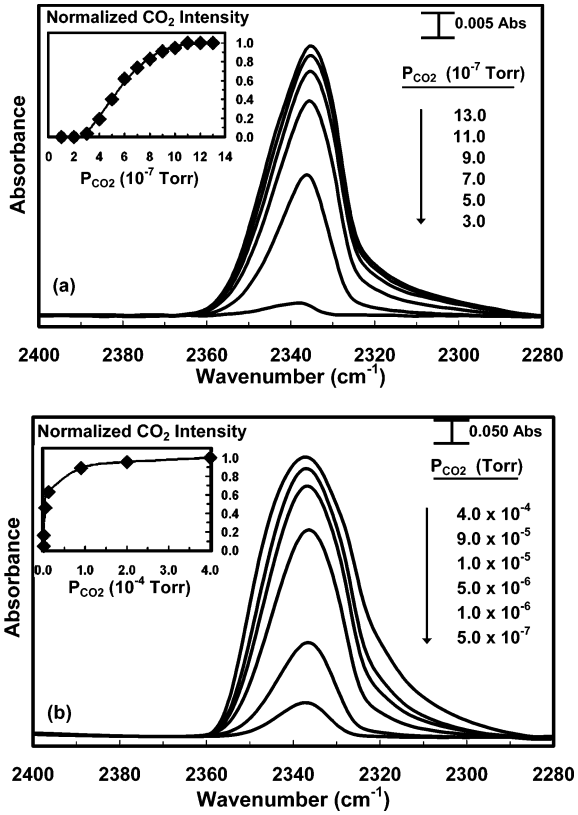

Figure 5. Infrared data for CO_2 physisorption in (a) $Zn_3[Co(CN)_6]_2$ at 77 K and in (b) $Co_3[Co(CN)_6]_2$ at 82 K. The normalized integrated CO_2 intensity as a function of the CO_2 pressure is displayed in the inset.

In previous works, CO_2 adsorption in heterogeneous carbon nanotube samples produced multiple peaks in the infrared spectra illustrating the different adsorption environments present in the sample.[6] Computational and experimental work were able to correlate the different infrared peaks with CO_2 adsorbed in different types of pores within the nanotube bundles.[6,20−24,29] The infrared spectra in Figure 5 only show a single peak that is fairly symmetric in nature. This result seems to indicate that a fairly homogeneous adsorption environment exists for CO_2 adsorbed in Prussian blue analogues, consistent with their highly crystalline structure. It also indicates that any small differences between the two types of pores present in these materials do not perturb the CO_2 ν_3 vibration in different manners. Overall, the infrared data suggest that the subtle differences between the two types of pores in the sample do not significantly affect CO_2 adsorption.

To examine the displacement of CO_2 by H_2, the sample was first saturated with CO_2 as shown in the insets of Figure 5a and b. The chamber was then backfilled with H_2 to increasingly higher pressures. Spectra at each pressure were taken after the system was allowed to reach equilibrium for 45−60 min. The results of this experiment are shown in Figure 6a. From the data, we can see that P_{H2}/P_{CO2} ratios as low as 100 do not cause significant amounts of exchange. At $P_{H2}/P_{CO2} = 1000$, the displacement is just starting to take place as indicated by a small decrease (~5%) seen in the CO_2 band intensity. As we approach P_{H2}/P_{CO2} of 10^6, approximately 19% of the preadsorbed CO_2 is displaced.

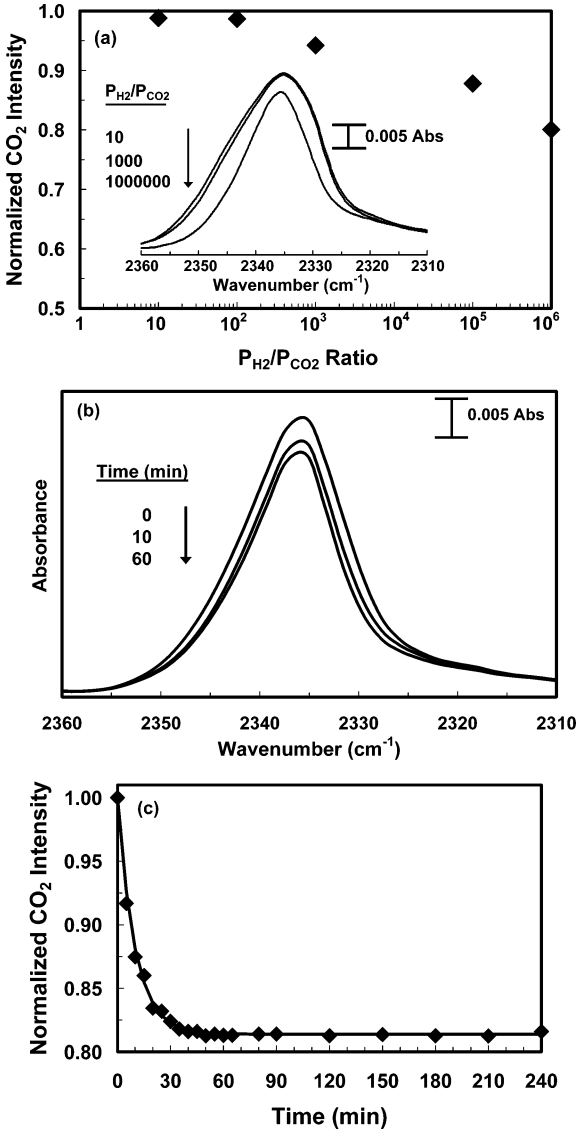

Figure 6. (a) Plot of the normalized integrated CO_2 intensity as a function of P_{H2}/P_{CO2} ratio for $Zn_3[Co(CN)_6]_2$. Inset shows comparison of IR spectra for the displacement of CO_2 by H_2 at various P_{H2}/P_{CO2} ratios. The experiment was performed at 77 K with an initial CO_2 pressure of 1.3×10^{-6} Torr. (b) CO_2 spectra during exchange with 1.0 Torr of H_2 at different time intervals at 77 K for $Zn_3[Co(CN)_6]_2$. (c) Plot of the normalized integrated CO_2 intensity as a function of time at 77 K for $Zn_3[Co(CN)_6]_2$. A solid line is a guide to the eye.

It is a bit surprising that H_2 is capable of displacing CO_2 on the basis simply of the isosteric heats of adsorption illustrated in Figure 4. The driving force for this exchange is clearly the large P_{H2}/P_{CO2} ratio which pushes the equilibrium of the system toward H_2 adsorption. Without going to extremely large P_{H2}/P_{CO2} ratios, there is no a driving force for displacement and CO_2 remains within the pores of the sample. The data in Figure 6a also show that the infrared intensity changes are fairly uniform indicating that CO_2 is homogeneously displaced from the pores of the sample. Overall, CO_2 and H_2 are competing for the same adsorption volume within the pores of the sample. These results are important for separation applications since they indicate that even though H_2 and CO_2 compete for the same adsorption volumes extremely high H_2 pressures are necessary for displacing CO_2.

Figure 6b shows the IR spectra during the exchange at 77 K in $Zn_3[Co(CN)_6]_2$ at different time intervals illustrating the kinetics of the exchange process. An intensity trace of these

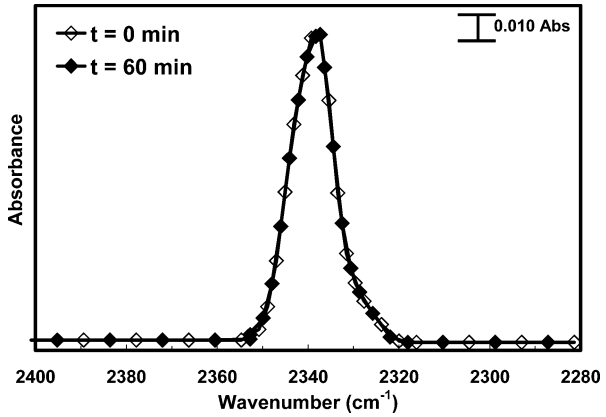

Figure 7. CO_2 ($P_{CO2} = 1.0$ Torr) spectra during exchange with 100 Torr of H_2 at 253 K for $Co_3[Co(CN)_6]_2$.

data is shown in Figure 6c. In Figure 6b, a loss of CO_2 intensity is seen at 2335 cm^{-1} which becomes more pronounced as time proceeds. After 60 min, no further decrease in the peak intensity can be observed indicating that the system has reached a new steady state. Data for the $Co_3[Co(CN)_6]_2$ sample show similar behavior. As a control experiment, FTIR studies were also performed without exposing the samples to H_2. We do not observe any intensity changes of the CO_2 band over the period of 240 min, confirming that preadsorbed CO_2 is only displaceable upon the introduction of gas-phase H_2.

Near Ambient CO_2 Displacement Experiments. Our CO_2 displacement studies indicate that ~19% of the preadsorbed CO_2 is exchanged with H_2 at 77 K (Figure 6c). To investigate if the displacement occurs at near ambient temperatures and pressures, we have conducted experiments at 253 K, with CO_2 partial pressure of 1.0 Torr and H_2 partial pressure of 100 Torr. This CO_2 pressure was chosen because it is the highest CO_2 pressure obtainable in our cell because of path length considerations. The H_2 pressure was chosen to make connections with Figure 6a. We are not able to go to much higher P_{H2}/P_{CO2} ratios at 253 K since the maximum pressure our cell can handle is 760 Torr.

In these experiments, none of the preadsorbed CO_2 is displaced by backfilling with H_2 on time scales of up to 60 min (Figure 7). This result agrees extremely well with our low-temperature data which also indicate that P_{H2}/P_{CO2} ratios of well over 100 are needed to drive the exchange. As a whole, our data point out that Prussian blue analogues have a preferential adsorption capacity for CO_2 over H_2. This preference is evident even at near ambient conditions and could possibly be exploited for separation applications (PSA) to obtain high-purity H_2 from the WGS reaction. The viability of these sorbents for PSA use would, of course, have to be examined in detail at process conditions realistic for real-world separation applications.

Summary. We have demonstrated the potential of H_2 storage in nanoporous Prussian blue analogues. These materials exhibited appreciable H_2 uptakes of 1.2−1.3 wt % at cryogenic temperatures and atmospheric pressure. The H_2 saturation coverage at 77 K was ~1.9 wt % above 6 atm for $Co_3[Co(CN)_6]_2$. They also possessed high adsorption capacity for CO_2 at ambient temperature and pressures up to 15 atm suggesting that they could be utilized as CO_2 sorbents for separation applications. Furthermore, infrared spectroscopic studies of CO_2 physisorption and its displacement by H_2 in dehydrated $Co_3[Co(CN)_6]_2$ and $Zn_3[Co(CN)_6]_2$ have been reported. The intensity changes of the 2335 cm^{-1} peak with H_2 exposure were due to CO_2 being displaced from the adsorption sites.

S.N. is supported by an RDS appointment sponsored by the U.S. Department of Energy. The authors thank Elizabeth Frommell for her assistance with XRD measurements. Reference in this work to any specific commercial product is to facilitate understanding and does not necessarily imply endorsement by the U.S. Department of Energy.

Supporting Information Available: Isosteres of CO_2 adsorption on $Co_3[Co(CN)_6]_2$ and $Zn_3[Co(CN)_6]_2$ at various coverages. This material is available free of charge via the Internet at http://pubs.acs.org.

References and Notes

(1) Kaye, S. S.; Long, J. R. *J. Am. Chem. Soc.* **2005**, *127*, 6506.
(2) Chapman, K. W.; Southon, P. D.; Weeks, C. L.; Kepert, C. J. *Chem. Commun.* **2005**, *26*, 3322.
(3) Hartman, M. R.; Peterson, V. K.; Liu, Y.; Kaye, S. S.; Long, J. R. *Chem. Mater.* **2006**, *18*, 3221.
(4) Culp, J. T.; Matranga, C.; Smith, M.; Bittner, E. W.; Bockrath, B. *J. Phys. Chem. B* **2006**, *110*, 8325.
(5) Mullica, D. F.; Milligan, W. O.; Beall, G. W.; Reeves, W. L. *Acta. Crystallogr.* **1978**, *B34*, 3558.
(6) Matranga, C.; Chen, L.; Smith, M.; Bittner, E.; Johnson, J. K.; Bockrath, B. *J. Phys. Chem. B* **2003**, *107*, 12930.
(7) Brown, D. B.; Shriver, D. F.; Schwartz, L. H. *Inorg. Chem.* **1968**, *7*, 77.
(8) Shriver, D. F.; Brown, D. B. *Inorg. Chem.* **1969**, *8*, 42.
(9) Kulesza, P. J.; Malik, M. A.; Denca, A.; Strojek, J. *Anal. Chem.* **1996**, *68*, 2442.
(10) Dailly, A.; Vajo, J. J.; Ahn, C. C. *J. Phys. Chem. B* **2006**, *110*, 1099.
(11) Khelifa, A.; Benchehida, L.; Derriche, Z. *J. Colloid Interface Sci.* **2004**, *278*, 9.
(12) Adamson, A. W. *Physical Chemistry of Surfaces*; John Wiley & Sons, Inc.: New York, 1982.
(13) Wang, Q. M.; Shen, D.; Bulow, M.; Lau, M. L.; Deng, S.; Fitch, F. R.; Lemcoff, N. O.; Semanscin, J. *Microporous Mesoporous Mater.* **2002**, *55*, 217.
(14) Choudhary, V.; Mayadevi, S. *Zeolites* **1996**, *17*, 501.
(15) Dunne, J. A.; Mariwala, R.; Rao, M.; Sircar, S.; Gorte, R. J.; Myers, A. L. *Langmuir* **1996**, *12*, 5888.
(16) Dunne, J. A.; Rao, M.; Sircar, S.; Gorte, R. J.; Myers, A. L. *Langmuir* **1996**, *12*, 5896.
(17) Kitaura, R.; Matsuda, R.; Kubota, Y.; Kitagawa, S.; Takata, M.; Kobayashi, T. C.; Suzuki, M. *J. Phys. Chem. B* **2005**, *109*, 23378.
(18) Herzberg, G. *Molecular Spectra and Molecular Structure II. Infrared and Raman Spectra of Polyatomic Molecules*; D. Van Nostrand Company, Inc.: New Jersey, 1960.
(19) Yamada, H.; Person, W. B. *J. Chem. Phys.* **1964**, *41*, 2478.
(20) Matranga, C.; Bockrath, B. *J. Phys. Chem. B* **2004**, *108*, 6170.
(21) Feng, X.; Matranga, C.; Vidic, R.; Borguet, E. *J. Phys. Chem. B* **2004**, *108*, 19949.
(22) Matranga, C.; Chen, L.; Bockrath, B.; Johnson, J. K. *Phys. Rev. B* **2004**, *70*, 165416.
(23) Matranga, C.; Bockrath, B. *J. Phys. Chem. B* **2005**, *109*, 4853.
(24) Matranga, C.; Bockrath, B. *J. Phys. Chem. B* **2005**, *109*, 9209.
(25) Heidberg, J.; Elstner, J.; Lassmann, W.; Folman, M. *J. Electron Spectrosc. Relat. Phenom.* **1993**, *64/65*, 883.
(26) Fastow, M.; Kozirovski, Y.; Folman, M. *J. Electron Spectrosc. Relat. Phenom.* **1993**, *64/65*, 843.
(27) Mawhinney, D. B.; Rossin, J. A.; Gerhart, K.; J.T. Yates, J. *Langmuir* **1999**, *15*, 4617.
(28) Goodman, A. L.; Campus, L. M.; Schroeder, K. T. *Energy Fuels* **2005**, *19*, 471.
(29) Yim, W. L.; Byl, O.; J. T. Yates, J.; Johnson, J. K. *J. Chem. Phys.* **2004**, *120*, 5377.